

Chiral Phosphoric Acids | Hot Paper |

 Experimental and Computational Studies on Regiodivergent Chiral Phosphoric Acid Catalyzed Cycloisomerization of Mupirocin Methyl EsterSibin Wang,^[a] Alonso J. Arguelles,^[b] Jia-Hui Tay,^[c] Miyuki Hotta,^[a] Paul M. Zimmerman,^{*[a]} and Pavel Nagorny^{*[a]}

Abstract: This article presents a new strategy for achieving regiocontrol over the *endo* versus *exo* modes of cycloisomerizations of epoxide-containing alcohols, which leads to the formation of five- or six-membered cyclic ethers. Unlike traditional methods relying on achiral reagents or enzymes, this approach utilizes chiral phosphoric acids to catalyze the regiodivergent selective formations of either tetrahydrofuran- or tetrahydropyran-containing products. By using methyl ester of epoxide-containing antibiotic mupirocin as the substrate, it is demonstrated that catalytic chiral phosphoric acids (*R*)-TCYP and (*S*)-TIPSY could be used to achieve

the selective formation of either the six-membered *endo* product (95:5 r.r.) or the five-membered *exo* product (77:23 r.r.), correspondingly. This cyclization was found to be unselective under the standard conditions involving various achiral acids, bases, or buffers. The subsequent mechanistic studies using state-of-the-art quantum chemical solutions provided the description of the potential energy surface, which is fully consistent with the experimental observations. Based on these results, highly detailed reaction paths are obtained and a concerted and highly synchronous mechanism is proposed for the formation of both *exo* and *endo* products.

Introduction

Three-membered cyclic ethers, called epoxides or oxiranes, are of great importance in both manmade applications and biosynthesis of natural products. An almost endless number of naturally occurring epoxides with a wide range of interesting biological activities are found in nature, which has further increased the interest of epoxides for biologists, pharmacologists, and synthetic chemists.^[1] Epoxides are highly strained heterocycles,^[2] which are relatively easy to synthesize in their enantiopure form by using asymmetric catalytic techniques such as the Sharpless asymmetric epoxidation of allylic alcohols,^[3] the Jacobsen epoxidation,^[4,5] the Shi epoxidation^[6,7] as well as a plethora of other methods.^[8,9] Thus, epoxide chemistry is dominated by ring-opening reactions, which relieve the vast potential energy that is captured in the ring strain.


Epoxide-based intermediates play an important role in the biosynthesis of various classes of natural products, and, in particular, cyclic ether-containing natural products such as polyether ionophores, the annonaceous acetogenins, and marine polyethers.^[10] In 1983, Cane, Celmer, and Westley proposed a unified stereochemical model of polyether antibiotic biogenesis, which implied that such natural products are formed through the cascade cyclization of the epoxide-containing biosynthetic precursors.^[11] Later, Nakanishi invoked the cascade cyclization of polyepoxide precursors in the biosynthesis of ladder polyether natural product brevetoxin B (Figure 1A).^[12] Since then, epoxide intermediates have become routinely proposed and observed in the biosynthesis of other cyclic ethers. The factors affecting the regioselectivity of the epoxide opening are not well understood, as such biosynthetic cascade reactions may often produce seemingly disfavored regioisomers. As demonstrated by Jamison and co-workers (Scheme 1C),^[13] the medium of such transformations plays an important role, and the use of water as the solvent was found to promote the formation of the kinetically less favored *endo* products. At the same time, enzymes are known to play an important role in controlling the selectivity of these reactions. For example, it was found that epoxide hydrolase Lsd19 is the enzyme that promotes 6-*endo*-cyclization in the biosynthesis of natural lasalocid A whereas the 5-*exo*-product isolasalocid A is formed under standard acidic conditions (Figure 1B).^[14]

Inspired by the aforementioned processes observed in nature, chemists have extensively used epoxyalcohol cycloisomerizations to generate various cyclic ethers (Scheme 1), in

[a] S. Wang, M. Hotta, Prof. Dr. P. M. Zimmerman, Prof. Dr. P. Nagorny
Chemistry Department, University of Michigan
930N. University Ave., Ann Arbor, MI 48109 (USA)
E-mail: paulzim@umich.edu
nagorny@umich.edu

[b] Dr. A. J. Arguelles
Eli Lilly and Company, 1500 South Harding Street, Indiana, IN 46221 (USA)

[c] Dr. J.-H. Tay
Corteva Agriscience, 9330 Zionsville Rd., Indianapolis, IN 46268 (USA)

 Supporting information and the ORCID identification number(s) for the author(s) of this article can be found under:
<https://doi.org/10.1002/chem.201905222>.

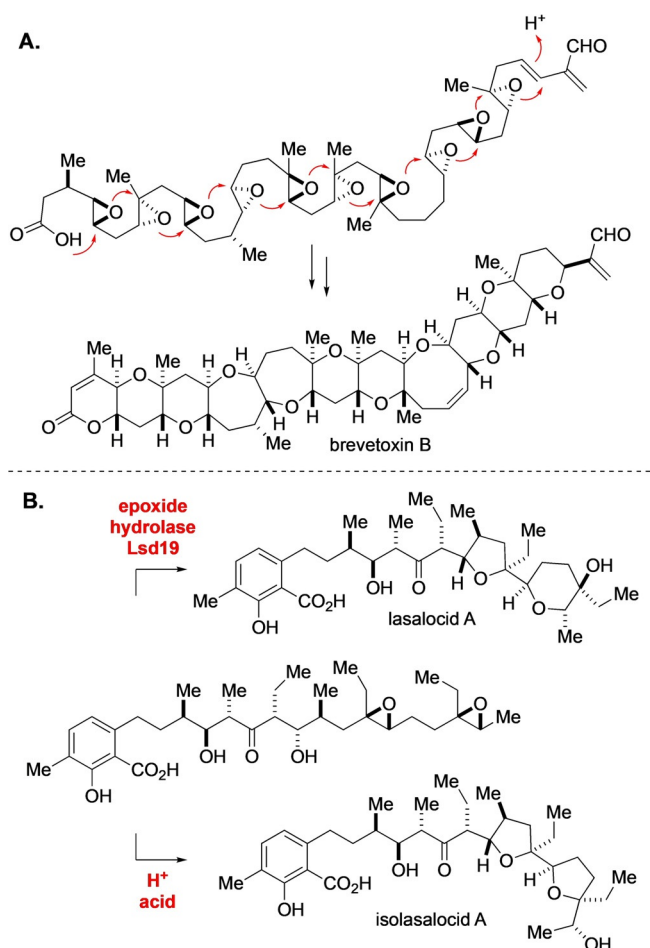
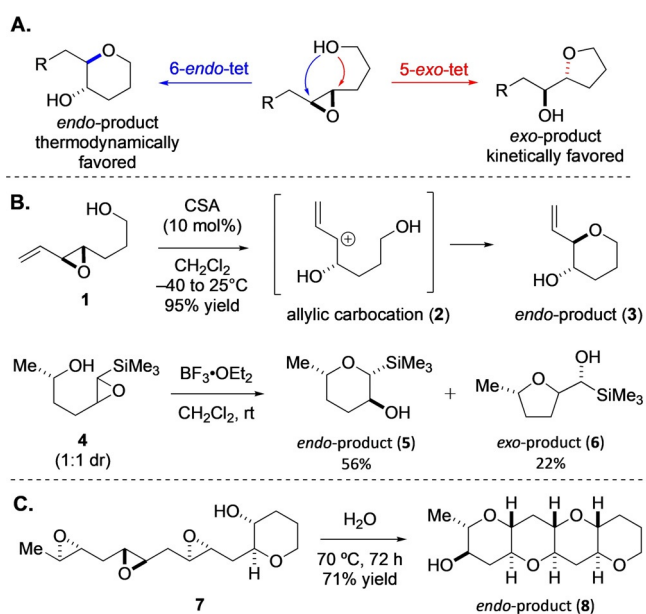


Figure 1. Biosynthetic epoxide cyclizations leading to the formation of cyclic ether containing natural products. A) Nakanishi's cascade hypothesis for the formation of brevetoxin A. B) Epoxide hydrolase Lsd19-controlled cyclization

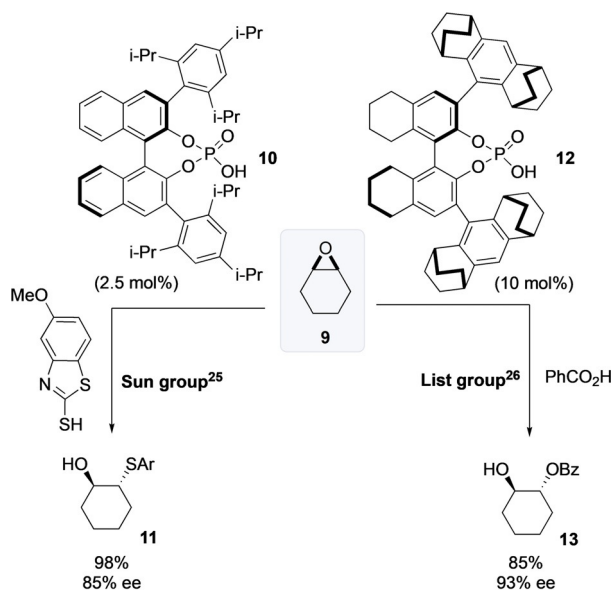


Scheme 1. A) The *endo* vs. *exo* modes of cyclization. B) Examples of substituent-directed *endo* cyclizations. C) *endo*-selective cascade cyclization by Jamison and co-workers.

particular tetrahydrofurans (THFs) and tetrahydropyrans (THPs). However, for such an approach to be a reliable strategy in the synthetic toolbox, effective ways to control the regioselectivity of the epoxide ring-opening (ERO) is mandatory. Baldwin's rules,^[15] a set of empirical generalizations that help discern kinetically favored intramolecular cyclizations, suggest that the regiochemistry of intramolecular ERO favors *exo* processes that proceed through a spiro transition state. Indeed, with a few exceptions, intramolecular ERO leads to the formation of five-membered rings (*exo* products) instead of six-membered rings (*endo* products; Scheme 1 A).^[16] For this reason, methods that facilitate *endo* control for intramolecular ERO are of high interest to synthetic chemists.

Most of the strategies developed to control the regiochemistry of intramolecular EROs have relied on the use of directing groups covalently present in the substrates. A variety of modifications have been developed, including alkenyl,^[17] alkynyl,^[18] alkyl,^[19] and silyl (Scheme 1 B).^[20] The majority of these methods justify their regioselectivity through electronic perturbations of the epoxide that stabilize the 6-*endo*-tet transition state (TS) or disfavor the 5-*exo*-tet TS. For instance, the Nicolaou group, pioneers of the regioselective ERO, used epoxyalcohols containing a simple vinyl substituent on the epoxide such as **1** to stabilize the nascent allylic carbocation intermediate **2**, which leads to *endo*-product **3** (Scheme 1 B).^[17c,d] Similarly, Schaumann and co-workers achieved a similar stereoelectronic bias by using silyl-substituted epoxides **4**, which preferentially produce *endo*-product **5** (Scheme 1 B).^[20b] In addition, the Jamison group discovered an effective strategy that is based on the use of neutral water in combination with a pre-installed THP template **7**, which results in the formation of poly-THP subunits such as **8** (Scheme 1 C).^[13,21]

These substrate-controlled strategies offered a breakthrough in intramolecular ERO. However, the use of covalently linked directing groups as the sole source of regiocontrol has some evident drawbacks. The most obvious one is that these methods are restricted in scope and tend to lack generality. In view of the recent successes in chiral catalyst-controlled selective functionalization of natural products,^[22] chiral catalyst-controlled regioselective intramolecular ERO could provide a more robust method that is applicable to a variety of substrates. Our group has a long-standing interest in the application of chiral phosphoric acids (CPAs) to control the regio- and stereoselective functionalization of natural products.^[23] In our recent efforts, we demonstrated that CPAs could mimic enzymatic processes and control the regioselectivity and/or stereoselectivity of acetalization,^[23d] spiroketalization,^[23c,e,f] and glycosylation^[23a,b] reactions. Inspired by the *endo* regiocontrol exhibited by the epoxide hydrolase Lsd19, which catalyzes the selective formation of lasalocid A rather than its kinetically favored regioisomer isolalocid A (Figure 1 B),^[19] we sought to investigate the possibility of controlling the formation of the *exo* and *endo* products through CPA catalysis. As an encouraging precedent, both the Sun and the List groups independently demonstrated the usefulness of CPAs **10** and **12** in the desymmetrization of *meso*-epoxide **9** with thiols and carboxylic acids as nucleophiles, respectively (Scheme 2).^[24,25] However,



Scheme 2. CPA-catalyzed epoxide desymmetrization by the Sun and List groups.

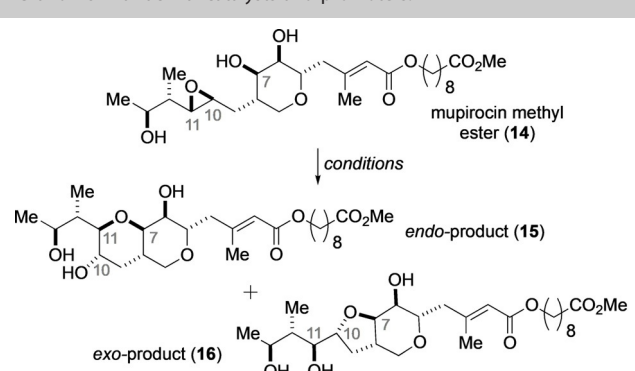
no applications of CPAs for controlling the regioselectivity of the epoxide opening have been reported to date.

This article describes the development and studies of CPA-controlled *endo*- and *exo*-selective cyclization of antibiotic mupirocin methyl ester, leading to the selective formation of either the THP- or THF-containing derivatives. To the best of our knowledge, this is the first example of a strategy that achieves regiocontrol by using chiral catalysts rather than achiral reagents or enzymes. The mechanisms of these transformations were investigated by using a combination of experimental techniques as well as computational methods based on the single-ended growing string (SE-GSM), a quantum chemical tool developed by the Zimmerman group.^[26] These mechanistic studies provide a description of the potential energy surface and suggest a concerted and highly synchronous mechanism for the formation of both the *exo* and *endo* products.

Results and Discussion

To test our hypothesis that CPAs could be used to control the regioselectivity of intramolecular ERO in a complex setting, we investigated the cyclization of the methyl ester of natural antibiotic mupirocin (**14**).^[27] The control experiments showed that the use of acidic, neutral, and basic conditions, which have been previously reported in the literature,^[28] resulted in either poor conversion or the unselective formation of both the *endo* and *exo* products (**15** and **16**, Table 1). The use of LiCl as the Lewis acid did not result in successful cyclization (entry 1), whereas ZnCl₂ and Sc(OTf)₃ catalyzed the unselective formation of **15** and **16** (entries 2 and 3). Interestingly, the suspension of **14** in deionized water underwent slow cyclization over the course of 4 days and provided a 71:29 mixture of **15/16** in 24% conversion (entry 4). The reaction rate could be significantly improved if pH 7 phosphate buffer was used instead

Table 1. Evaluation of mupirocin methyl ester (**14**) cyclization leading to **15** and **16** with achiral catalysts and promoters.

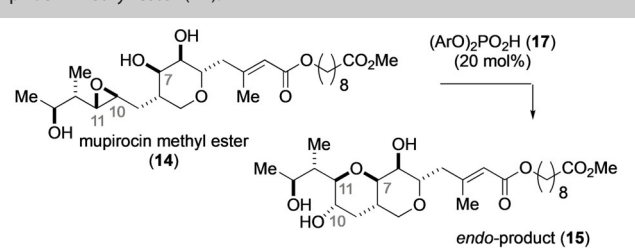


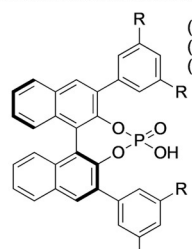
Entry	Catalyst/conditions	Solvent	Time	Conversion [%]	15/16 ^[b]
1 ^[a]	LiCl	CH ₂ Cl ₂	12 h	< 5	–
2 ^[a]	ZnCl ₂	CH ₂ Cl ₂	12 h	82	48:52
3 ^[c]	Sc(OTf) ₃	CH ₂ Cl ₂	12 h	77	57:43
4 ^[d]	–	H ₂ O	4 d	24	71:29
5	KH ₂ PO ₄ buffer (pH 7)	H ₂ O	4 d	> 98	48:52
6 ^[e]	Cs ₂ CO ₃	CH ₂ OH	4 d	–	–
7 ^[f]	LiHMDS	THF	4 d	–	–
8 ^[g]	(<i>p</i> -NO ₂ -C ₆ H ₄ O) ₂ PO ₂ H	CH ₂ Cl ₂	5 d	> 98	70:30

[a] Conditions: **14** (0.02 mmol), catalyst (20 mol %), CH₂Cl₂ (0.01 M). [b] Determined by RP HPLC. [c] Conditions: catalyst (20 mol %), CH₂Cl₂ (0.2 M). [d] 70 °C. [e] Cs₂CO₃ (10 equiv), CH₂Cl₂ (0.02 M). [f] LiHMDS (3 equiv), CH₂Cl₂ (0.01 M). [g] Catalyst (20 mol %), CH₂Cl₂ (0.2 M).

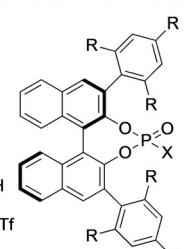
(entry 5); however, this reaction proceeded with no selectivity and produced an equimolar mixture of **15** and **16**. The use of more basic conditions did not produce the desired cyclization products (entries 6 and 7). However, using catalytic amounts of the acidic phosphoric acid (*p*-NO₂-C₆H₄O)₂PO₂H, resulted in complete conversion of mupirocin methyl ester **14**, and low levels of *endo* selectivity were observed (entry 8). This suggests that, contrary to what might be expected by Baldwin's rules, phosphoric acid catalysis has small inherent *endo* selectivity for the intramolecular ERO of mupirocin methyl ester, but high selectivity for either **15** or **16** is unlikely to be achieved when using achiral catalysts or conditions.

Following these control studies, we then investigated if the use of CPAs could further enhance the formation of **15** or even reverse the observed trend and favor the *exo*-product **16**. To this end, we screened a number of BINOL-derived CPAs (Table 2).^[29] We selected methylene chloride dried with 4 Å MS as the starting solvent owing to its excellent solvating properties and good compatibility with phosphoric acid catalysis. Subsequently, we evaluated an array of BINOL-based CPAs (see Tables S2–S6 in the Supporting Information for the full list of catalysts and conditions). Encouragingly, we found that the axial chirality of the BINOL backbone had a significant impact on the regioselectivity of this transformation, with (*R*)-CPAs consistently favoring *endo*-product **16** formation more than the (*S*)-enantiomers (Table 2, entries 1–9). Although CPAs bearing 3,5-substituted aryl groups at the 3,3'-positions of the BINOL scaffold were not effective (catalysts **17 a–c**, entries 1–5), the 2,4,6-substituted CPAs such as (*R*)-TRIP (**17 d**) and (*R*)-TCYP

Table 2. Development of CPA-controlled *endo*-selective cyclization of mupirocin methyl ester (**14**).




(*S*)-**17a**, R= Cl
(*S*)-**17b**, R= CF₃
(*S*)-**17c**, R= SF₅



(*R*)-**17d**, R= *i*-Pr, X=OH
(*R*)-**17e**, R=Cy, X=OH
(*R*)-**17f**, R= *i*-Pr, X=NHTf

Entry ^[a]	Catalyst	Solvent ^[b]	Conversion [%]	15/16 ^[b]
1	(<i>S</i>)- 17a	CH ₂ Cl ₂	> 98	66:34
2	(<i>R</i>)- 17a	CH ₂ Cl ₂	> 98	74:26
3	(<i>S</i>)- 17b	CH ₂ Cl ₂	95	62:38
4	(<i>S</i>)- 17c	CH ₂ Cl ₂	> 98	66:34
5	(<i>R</i>)- 17c	CH ₂ Cl ₂	> 98	73:27
6	(<i>S</i>)- 17d	CH ₂ Cl ₂	> 98	57:43
7	(<i>R</i>)- 17d	CH ₂ Cl ₂	> 98	93:7
8	(<i>S</i>)- 17e	CH ₂ Cl ₂	> 98	45:55
9	(<i>R</i>)- 17e	CH ₂ Cl ₂	> 98	94:6
10	(<i>R</i>)- 17f	CH ₂ Cl ₂	> 98	48:52
11 ^[c]	(<i>R</i>)- 17e	CH ₂ Cl ₂	67	90:10
12 ^[c]	(<i>R</i>)- 17e	CyH	39	77:23
13 ^[c]	(<i>R</i>)- 17e	PhCF ₃	> 98	92:8
14 ^[c]	(<i>R</i>)- 17e	PhMe	> 98	95:5
15 ^[c,d]	(<i>R</i>)- 17e	PhMe	> 98	97:3
16 ^[c,e]	(<i>R</i>)- 17e	PhMe	> 98	95:5
17 ^[c,f]	(<i>R</i>)- 17e	PhMe	> 98	95:5
18 ^[c,g]	(<i>R</i>)- 17e	PhMe	93%	93:7

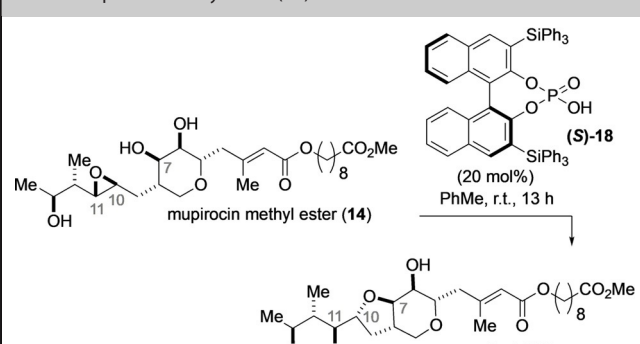
[a] Conditions: **14** (0.02 mmol), solvent (0.2 M), 4 Å molecular sieves (MS), room temperature, 12 h. [b] Determined by RP HPLC. [c] Reactions were performed without 4 Å MS. [d] Reaction was performed with 100 mol% of the catalyst. [e] Reaction was performed with 10 mol% of the catalyst. [f] Reaction was performed with 5 mol% of the catalyst on a 0.20 mmol scale for 18 h. [g] Reaction was performed with 5 mol% of the catalyst in the presence of 5 mol% of water.

(**17e**) were found to be superior catalysts for the formation of *endo*-product **15** (entries 6–10).

As before, the (*S*)-enantiomers of **17d** and **17e** did not provide good selectivities and were not further investigated. Similarly, the use of more acidic *N*-triflyl phosphoramidate **17f** did not result in a selective reaction, and no further attempts to investigate this class of Brønsted acids was pursued. Other Brønsted acids and hydrogen bond donor (HBD) catalysts were also tested without success (see the Supporting Information, Table S5). Based on these results, catalyst **17e** was selected and the reaction conditions were further optimized (entries 11–17). The evaluation of other non-polar non-coordinating solvents in the absence of 4 Å MS led to the selection of toluene as the solvent of choice, which resulted in an increase

in regioselectivity (95:5, entry 14). Under these optimized conditions, we found that the catalyst loading could be lowered to 5 mol% on a larger reaction scale (0.20 mmol) with minimal detriment to the regioselectivity (entry 17). As expected, an increase in the catalyst loading results in faster reaction times and higher **15/16** ratios (entry 16). In addition, this reaction tolerated the presence of 5 mol% of water without any significant effect on the selectivity (entry 18).

Having been successful in finding conditions for the preparation of the *endo*-product **15** with excellent conversion and regioselectivity, we conjectured that we could bias the selectivity towards the formation of the *exo*-product **16** through the judicious choice of a CPA, especially after having observed that in all cases BINOL-derived catalysts with (*S*)-chirality gave better *exo* selectivity than achiral phosphoric acids (Table 2, entries 1, 3, 4, 6, 8, compared with Table 1, entry 7). To this end, we evaluated (*S*)-CPAs (see the Supporting Information, Tables S4–S6) using toluene as the solvent and identified (*S*)-TIPSY (**18**) as the catalyst that enhances the formation of the *exo*-product **16** (Table 3). The selectivity of this transformation was found to be concentration dependent, and gradual decrease of the concentration (0.2 M to 0.01 M) led to the enhancement of the *exo/endo* selectivity to 74:26 (entries 1–5). To our delight, we found that the use of 5 mol% of (*S*)-TIPSY does not erode the selectivity, and 75% of the *exo*-product **16** was obtained after stirring the reaction mixture for 72 h (77:23, Table 3, entry 6). Unlike the reaction with (*R*)-TCYP (Table 2, entry 19), this transformation was highly sensitive to the presence of water as the presence of even 5 mol% of water resulted in an unselective pathway and slower reaction rates (Table 3, entry 7).

Table 3. Development of (*S*)-TIPSY (**18**)-controlled *exo*-selective cyclization of mupirocin methyl ester (**14**).


Entry ^[a]	Concentration [M]	Loading [mol %]	Conversion [%]	15/16 ^[b]
1	0.5	20	94	55:45
2	0.2	20	90	48:52
3	0.1	20	85	38:62
4	0.025	20	83	35:65
5	0.01	20	95	26:74
6 ^[c]	0.01	5	77	23:77
7 ^[d]	0.01	5	44	45:55

[a] Conditions: **14** (0.02 mmol), toluene, room temperature, 12 h. [b] Determined by ¹H NMR spectroscopy. [c] **14** (0.2 mmol), toluene, room temperature, 72 h. [d] This reaction was attempted in the presence of 5 mol% of H₂O.

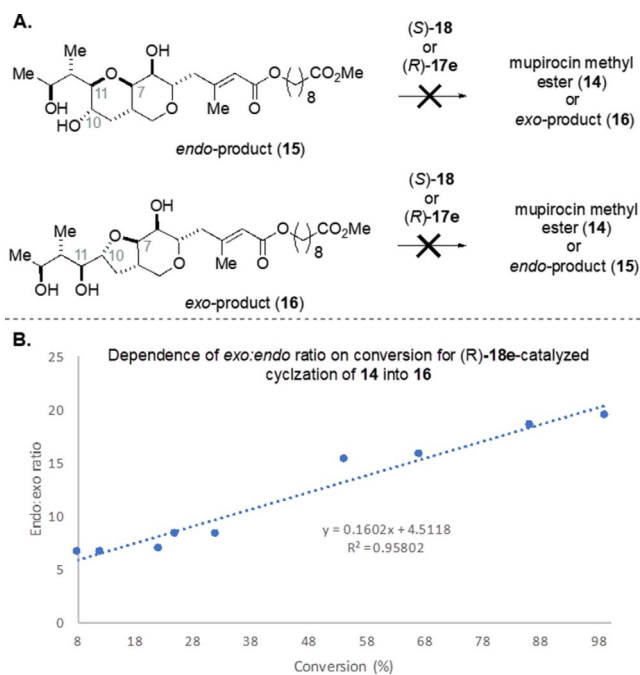


Figure 2. A) Control experiments to probe the isomerization of **15** and **16** under the reaction conditions. B) Dependence of the *endo/exo* selectivity on reaction progression for the (*R*)-**17e** catalyzed cyclization of **14**.

With the catalyst-controlled pathways leading to both **15** and **16**, some experimental studies to probe the potential reaction mechanism were performed (Figure 2A). To rule out the CPA-catalyzed equilibration, both **15** and **16** were subjected to (*R*)-**17e** and (*S*)-**18**, and no isomerization, retrocyclization, or material degradation was noted at room temperature. The selectivities of the cyclizations leading to both *endo*-product (**15**) and *exo*-product (**16**) were found to be conversion-dependent and increased with the progression of these reactions (Figure 2B and Supporting Information, Tables S7 and S8). However, the addition of 0.5 equivalents of either the *endo*- or *exo*-products **15** or **16** to the initial reaction mixture did not affect the selectivity versus conversion profiles. Similarly, neither **15** nor **16** acted as the catalysts when stirred with mupirocin methyl ester (**14**). These results coupled with the observation that catalytic quantities of water diminish the reaction selectivity strongly suggest the formation of hydrogen-bond complexes between **14** and catalysts (*R*)-**17e** or (*S*)-**18**.

Based on these experimental observations, we turned to computation to help explain the reaction mechanism and observed selectivities.^[30] In particular, Zimmerman group's reaction exploration tools were used to facilitate the accurate and fast search of relevant reactions paths and transition states.^[25] These tools have previously been used in the elucidation of fine mechanistic details of phosphoric acid-catalyzed spiroketalizations, glycosylations, and intramolecular aza-Michael reactions.^[23b,c,31] Here, the single-ended growing string method (GSM) was employed to detail the mechanism of phosphoric acid-catalyzed intramolecular ERO.

To alleviate computational costs, a truncated model of the mupirocin methyl ester (**20**) was used alongside biphenyl

phosphoric acid (**BPA**, **19**) as the catalyst (Figure 3). Given that CPAs possess both Brønsted acidic and Lewis basic sites in proximity, it is possible that CPAs simultaneously activate the electrophilic epoxide and the nucleophilic alcohol.^[25d,32] Several arrangements that allow such concerted operation were modeled, leading to the products **21** (*exo* reaction) and **22** (*endo* reaction).

These simulations (Figure 3) revealed that the formation of a substrate-BPA complex [**20-BPA**] was thermodynamically favored by 3.5 kcal mol⁻¹ over separated reactant/catalyst, giving three hydrogen bonds between the C6, C7, and C13 hydroxy groups and the phosphoric acid. Upon transforming this complex, the *endo*-product **22** was found to be 12.6 kcal mol⁻¹ downhill from the substrate-BPA complex [**20-BPA**], making it preferred by 5.1 kcal mol⁻¹ over the *exo* product. Concerted reaction pathways for the formation of *endo* and *exo* products were readily found by using GSM (Figure 3). These revealed that the preferred regioisomeric pathways, although topologically distinct, shared almost identical activation barriers of around 19.1 kcal mol⁻¹. The *endo* pathway was preferred minutely by 0.16 kcal mol⁻¹, a number that, although within the error of the computational methods, agrees with the small intrinsic *endo* selectivity that is observed with achiral phosphoric acids experimentally (Figure 3, TS_{endo} vs. TS_{exo} and Table 1, entry 7). An alternative mechanism through epoxide opening and involving a phosphate intermediate^[23b,31] was ruled out because the barrier was substantially higher (≈ 8.3 kcal mol⁻¹, TS_p) than the concerted pathways.

The reverse reactions for the concerted mechanism have activation barriers of 36.0 and 32.1 kcal mol⁻¹ for *endo* and *exo* product formation, respectively, indicating the transformation is irreversible at room temperature. This is consistent with the observation that no interconversion was observed between the *exo* product (**21**) or *endo* product (**22**) in the control experiments (Figure 2A). As mentioned earlier, the preferred *endo* and *exo* pathways are close in energy and share some common features. For instance, in both cases, the hydroxyl group at C13 is needed to serve as a proton donor/acceptor relay for the concerted pathway to be operative (Figure 4). Indeed, models lacking this functional group require a stepwise sequence of events (protonation, rotation, and cyclization) to yield the product and have a higher activation barrier. Another shared feature for this pathway is that protonation of the epoxide (red arrows) and cyclization (blue arrows) occur simultaneously in the TS. There are, however, important differences between the *endo* and *exo* pathways. The geometrical demands of 5-*exo*-tet cyclizations require a more closed and tight transition state, and the C13 hydroxyl group serves as a relay to protonate the epoxide, whereas the phosphoric acid activates the C7 alcohol. On the other hand, the 6-*endo*-tet mechanism involves a more open transition state, and the C13 hydroxyl group serves as a relay to activate the C7 alcohol, whereas the phosphoric acid protonates the epoxide directly.

The quadrant-based analysis, developed by the groups of Himo and Terada to explain the selectivity of BINOL-based CPAs,^[33] has been previously used to describe the steric profile imposed by these acids (Figure 4A).^[23c] Herein, we use a similar

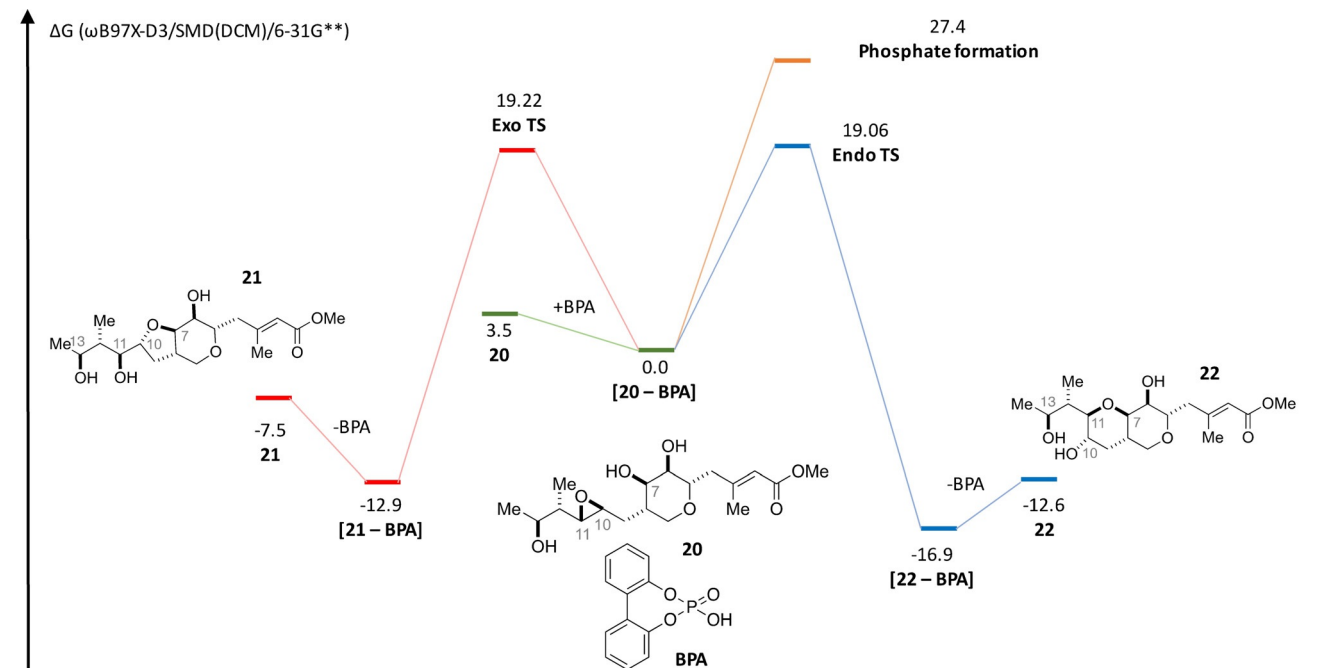
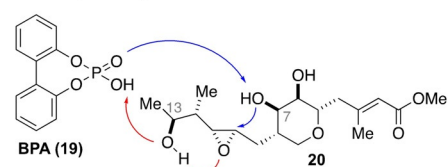
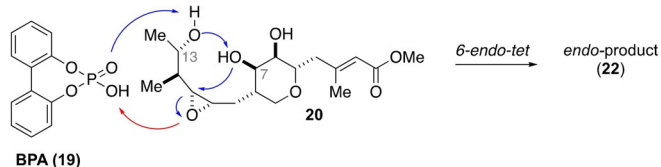
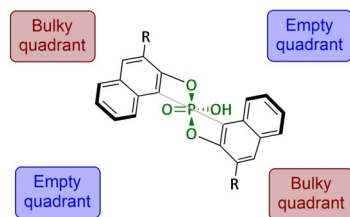
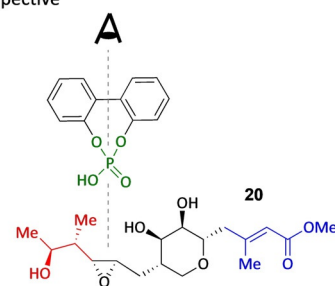
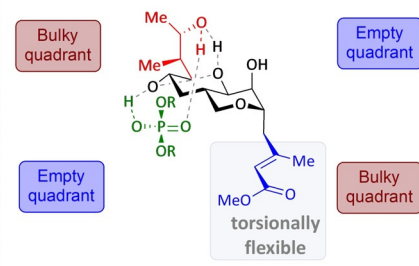
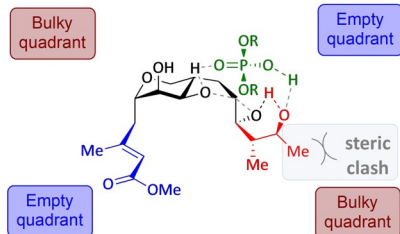
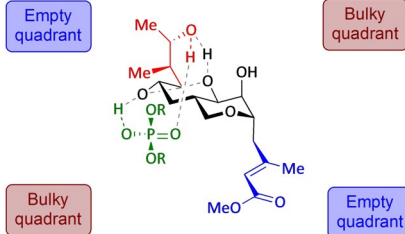
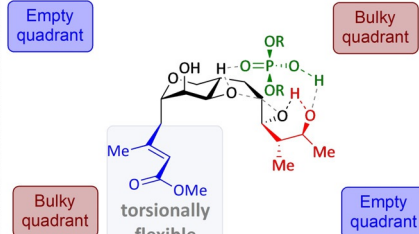
A. *exo*-pathwayB. *endo*-pathway

Figure 3. Energy diagram for the intramolecular ERO of a truncated mupirocin model.

A. Quadrant analysis for (*R*)-BINOL-derived CPAs

B. Perspective

C. *Endo*-cyclization TS with (*R*)-CPAD. *Exo*-cyclization TS with (*R*)-CPAE. *Endo*-cyclization TS with (*S*)-CPAF. *Exo*-cyclization TS with (*S*)-CPAFigure 4. Quadrant-based perspective for key TSs. A) Quadrant analysis for (*R*)-BINOL-derived CPAs. B) Perspective taken. C) 6-*Endo*-tet pathway in a (*R*)-CPA quadrant framework. D) 5-*Exo*-tet pathway in a (*R*)-CPA quadrant framework. E) 6-*Endo*-tet pathway in a (*S*)-CPA quadrant framework. F) 5-*Exo*-tet pathway in a (*S*)-CPA quadrant framework. The biphenyl backbone of the catalyst is omitted for clarity.

analysis to explain the observed selectivity pattern. This qualitative model uses the TS for *endo* and *exo* cyclization obtained with BPA (Figures 3, 4B) as a template to juxtapose the steric profile of (*R*)- or (*S*)-BINOL-derived CPAs. Figure 4C and E show that the 6-*endo*-tet pathway leading to **22** would not have significant contacts with either (*R*)- or (*S*)-CPAs, and most of the interactions are with torsionally flexible parts of the substrate, colored blue in Figure 4. This is consistent with the more open and flexible TS compared with the 5-*exo*-tet pathway and suggests that the choice of chirality of the CPA does not have a drastic impact on the 6-*endo*-tet cyclization activation barrier. On the other hand, the tighter TS of the 5-*exo*-tet mechanism places an inflexible and bulky group (colored in red in Figure 4) in the bottom right quadrant pointing towards the phosphoric acid (Figure 4D and F). This implies that (*R*)-BINOL-derived CPAs would disfavor the *exo* pathway owing to steric clashes in this quadrant. On the other hand, CPAs with (*S*)-chirality, which have an inverse steric profile, would not suffer from these interactions and would therefore have lower barriers for the formation of *exo*-product **21** (Figure 4D). Taking both considerations together, this model explains why catalysts with (*R*)-chirality favor *endo* product formation more than those with (*S*)-chirality and is in agreement with the experimental results (Table 2 and Table 3).

Conclusion

We have developed a catalyst-controlled method for the regioselective intramolecular epoxide ring-opening of mupirocin derivatives. After an extensive screening, we found that (*R*)-TCYP could catalyze the formation of *endo*-product **15** in 95:4 r.r., whereas (*S*)-TIPSY yielded the *exo*-product **16** in 77:23 r.r. Importantly, we investigated the mechanism by using state-of-the-art quantum chemical solutions developed by the Zimmerman group. We found that our method could rapidly describe a potential energy surface fully consistent with the experimental observations. On the basis of our results, we postulate that a concerted and highly synchronous mechanism is likely for this reaction. We obtained highly detailed reaction paths for the formation of *exo* and *endo* products, which, although similar in activation barrier, showed key structural dissimilarities that helped us establish the origin of the regiocontrol of these reactions; this is likely due to hindrance of the 5-*exo*-tet cyclization caused by steric clashes of the epoxide alkyl substituents with the 3- and 3'-substituents of BINOL-derived CPAs with (*R*)-chirality. Catalyst-controlled regiodivergent methods for epoxide opening are scarce but synthetically useful and versatile. We hope that our mechanistic insights can assist in developing this methodology further to make it more broadly applicable to cases useful to the organic chemist. We also envision that CPAs could be broadly applied to affect other intramolecular ERO reactions such as the ones depicted in Figure 1 and Scheme 1, and these studies are currently ongoing in our laboratories.

Experimental Section

General methods and materials

All reactions were carried out under an atmosphere of nitrogen in flame- or oven-dried glassware with magnetic stirring. Mupirocin was purchased from Sigma–Aldrich and used as such. Chiral phosphoric acids (*R*)-**17e** and (*S*)-**18** are commercially available or could be synthesized by using known procedures. Deionized water was used in the preparation of all aqueous solutions and for all aqueous extractions. Solvents used for extraction and chromatography were ACS or HPLC grade. Purification of reaction mixtures was performed by flash chromatography using a SiliCycle SiliaFlash P60 (230–400 mesh). Diastereomeric ratios were determined by RP HPLC analysis by using a Shimadzu SBM-20A Separations Module with a photodiode array detector equipped with C18 Nova-Pack® column (60 Å, 4 mm, 3.9×150 mm). All spectra were recorded with Varian vnmrs 700 (700 MHz), Varian vnmrs 500 (500 MHz), Varian MR400 (400 MHz), Varian Inova 500 (500 MHz) spectrometers and chemical shifts (δ) are reported in parts per million (ppm) and referenced to the ¹H signal of the internal tetramethylsilane according to IUPAC recommendations. Data are reported as (br=broad, s=singlet, d=doublet, t=triplet, q=quartet, qn=quintet, sext=sextet, m=multiplet; coupling constant(s) in Hz; integration). High-resolution mass spectra (HRMS) were recorded with Micro-mass AutoSpecUltima or VG (Micromass) 70–250-S Magnetic sector mass spectrometers at the University of Michigan mass spectrometry laboratory. Infrared (IR) spectra were recorded as thin films on NaCl plates with a PerkinElmer Spectrum BX FTIR spectrometer and are reported in wavenumbers (cm⁻¹).

Computational details

All quantum chemical calculations were performed by using the Q-Chem 4.3 package.^[34] Geometry optimizations were evaluated by using the B97-D density functional^[35] using the double- ζ - quality basis set with polarization functions on all atoms, 6-31G**.^[36] Pictorial representations of important stationary points were generated with the Discovery Studio 4.1 Visualizer. The electronic contributions to the Gibbs free energy of all stationary points were computed through solvent-corrected (dichloromethane) single-point energies by using the SMD model.^[37] For these calculations, the ω B97X-D3 exchange functional^[38] was employed with a 6-31G** basis set. The final Gibbs free energy values were obtained by correcting the electronic free energy with the enthalpic and entropic contributions from vibrations, rotations, and translations at 298.15 K. These frequency computations were performed by using the B97-D functional and 6-31G** basis set.

Synthesis and characterization

Synthesis of mupirocin methyl ester 14: Mupirocin (2.0 g, 4.0 mmol) was initially dissolved in toluene (16 mL) and methanol (4 mL). Then, trimethylsilyldiazomethane (2.4 mL, 4.8 mmol, 1.2 equiv) was added dropwise. The reaction mixture was stirred for 1 h at room temperature under N₂. After the reaction is completed, the reaction mixture was diluted with EtOAc (15 mL), quenched with 10% v/v AcOH (15 mL) and extracted with EtOAc (15 mL×3). The combined organic extract was washed with brine and dried with Na₂SO₄ and concentrated in vacuo to obtain a yellow oil. The crude mixture was purified by recrystallization in hexane (10 mL) and diethyl ether (20 mL) and filtered through a Buchner funnel to afford **14** (1.93 g, 85%) as a white solid. ¹H NMR (700 MHz, CDCl₃): δ = 5.76 (d, *J* = 1.6 Hz, 1H), 4.07 (t, *J* = 6.7 Hz, 2H),

3.93 (s, 1H), 3.86 (d, $J=3.1$ Hz, 1H), 3.82 (t, $J=6.4$ Hz, 1H), 3.76 (td, $J=8.7, 3.4$ Hz, 1H), 3.67 (s, 3H), 3.56 (dd, $J=11.7, 2.8$ Hz, 1H), 3.48 (d, $J=7.7$ Hz, 1H), 2.80 (ddd, $J=6.9, 5.0, 2.2$ Hz, 1H), 2.70 (dd, $J=8.0, 2.2$ Hz, 1H), 2.61–2.54 (m, 1H), 2.38 (s, 1H), 2.33–2.18 (m, 8H), 2.01 (dq, $J=7.2, 3.9$ Hz, 1H), 1.79–1.67 (m, 2H), 1.40–1.27 (m, 10H), 1.22 (d, $J=6.3$ Hz, 3H), 0.94 ppm (d, $J=7.0$ Hz, 3H); ^{13}C NMR (176 MHz, CDCl_3): $\delta=174.4, 166.7, 156.6, 117.6, 77.2, 77.0, 76.8, 74.8, 71.4, 70.4, 69.0, 65.3, 63.8, 61.3, 55.6, 51.5, 42.84, 42.82, 39.5, 34.1, 31.5, 29.1, 29.03, 29.01, 28.6, 25.9, 24.9, 20.8, 19.0, 12.7$ ppm; IR (thin film): 3564, 3399 (br), 1737, 1712, 1647, 1218, 1142, 1110, 1075, 941, 922, 890, 814, 754, 669 cm^{-1} ; $[\alpha]_{\text{D}}^{25}=-9.4$ ($c=2.06$, CHCl_3); HRMS (ESI+) (m/z): $[M+\text{Na}]^+$ calcd for $\text{C}_{27}\text{H}_{46}\text{O}_9$: 537.3040; found: 537.3014.

Endo-selective cyclization leading to 15: To a flame-dried, N_2 -flushed 1-dram vial, a stir bar and mupirocin methyl ester 14 (104 mg, 0.2 mmol) were added. This was followed by the addition of chiral phosphoric acid (*R*)-17e (10 mg, 0.01 mmol, 0.05 equiv) and dissolved in toluene (1.0 mL, 0.2 M). The reaction was stirred for 18 h at room temperature before being concentrated on a rotary evaporator and purified by chromatography on silica gel by using 10:9:1 hexanes/dichloromethane/methanol ($R_f=0.2$). This provided 97 mg of purified *endo*-product 15 in 93% yield. ^1H NMR (700 MHz, CDCl_3): $\delta=5.69$ (d, $J=1.9$ Hz, 1H), 4.22 (ddd, $J=10.0, 5.3, 1.4$ Hz, 1H), 4.06 (t, $J=6.7$ Hz, 2H), 3.79 (p, $J=6.5$ Hz, 1H), 3.74 (t, $J=2.0$ Hz, 1H), 3.65 (s, 3H), 3.63 (d, $J=2.0$ Hz, 1H), 3.60 (ddd, $J=16.2, 10.8, 5.1$ Hz, 2H), 3.33–3.24 (m, 2H), 2.57 (dd, $J=14.2, 9.9$ Hz, 1H), 2.28 (t, $J=7.5$ Hz, 2H), 2.24–2.17 (m, 5H), 2.17–2.08 (m, 1H), 2.01 (dt, $J=11.7, 3.9$ Hz, 1H), 1.93 (pd, $J=7.1, 1.8$ Hz, 1H), 1.66–1.55 (m, 5H), 1.37–1.27 (m, 10H), 1.25 (d, $J=6.3$ Hz, 3H), 0.96 ppm (d, $J=7.1$ Hz, 3H); ^{13}C NMR (176 MHz, CDCl_3): $\delta=174.31, 166.40, 155.05, 118.27, 82.03, 77.05, 75.94, 70.15, 69.11, 66.34, 64.16, 63.93, 53.41, 51.45, 39.96, 39.86, 34.58, 34.05, 32.90, 29.08, 29.03, 29.00, 28.62, 25.91, 24.87, 22.16, 18.28, 10.78$ ppm; IR (thin film): 3407 (br), 2930, 2856, 1713, 1646, 1436, 1223, 1149, 1095, 1056, 997, 914, 862, 808, 753, 610 cm^{-1} ; $[\alpha]_{\text{D}}^{25}=-8.5$ ($c=1.91$, CHCl_3); HRMS (ESI+) (m/z): $[M+\text{Na}]^+$ calcd for $\text{C}_{27}\text{H}_{46}\text{O}_9$: 537.3040; found: 537.3054.

Exo-selective cyclization leading to 16: To a flame-dried, N_2 -flushed 1-dram vial, a stir bar and mupirocin methyl ester 14 (100 mg, 0.2 mmol) were added. This was followed by the addition of chiral phosphoric acid (*S*)-18 (10 mg, 0.01 mmol, 0.05 equiv) and dissolved in toluene (20 mL, 0.01 M). The reaction was stirred for 72 h at room temperature before being concentrated on a rotary evaporator and purified by chromatography on silica gel by using 10:9:1 hexanes/dichloromethane/methanol ($R_f=0.2$). This provided 77 mg of purified *exo*-product 16 in 77% yield. ^1H NMR (700 MHz, CDCl_3): $\delta=5.70$ (s, 1H), 4.28 (ddd, $J=9.4, 5.9, 3.3$ Hz, 1H), 4.14 (ddd, $J=9.5, 5.4, 1.8$ Hz, 1H), 4.07 (t, $J=6.7$ Hz, 2H), 4.03–3.98 (m, 2H), 3.91 (dd, $J=9.5, 3.3$ Hz, 1H), 3.89–3.83 (m, 1H), 3.66 (s, 3H), 3.64 (dd, $J=11.3, 3.1$ Hz, 1H), 2.50 (dd, $J=14.2, 9.4$ Hz, 1H), 2.41 (ddq, $J=17.2, 11.5, 5.4$ Hz, 1H), 2.30 (t, $J=7.5$ Hz, 2H), 2.25 (dd, $J=14.1, 5.4$ Hz, 1H), 2.20 (d, $J=1.3$ Hz, 3H), 1.91 (dt, $J=11.6, 5.9$ Hz, 1H), 1.80 (td, $J=12.1, 9.8$ Hz, 1H), 1.61 (hept, $J=6.8$ Hz, 5H), 1.49 (dp, $J=9.1, 7.1$ Hz, 1H), 1.38–1.27 (m, 10H), 1.19 (d, $J=6.2$ Hz, 3H), 0.81 ppm (d, $J=6.9$ Hz, 3H); ^{13}C NMR (176 MHz, CDCl_3): $\delta=174.29, 166.42, 155.15, 118.27, 81.14, 80.59, 77.29, 76.16, 72.24, 68.98, 65.62, 63.88, 51.45, 41.98, 41.40, 36.27, 34.06, 29.09, 29.03, 29.01, 28.63, 26.36, 25.92, 24.88, 20.93, 18.38, 12.54$ ppm; IR (thin film): 3407 (br), 2929, 2856, 1714, 1646, 1436, 1223, 1149, 1059, 993, 913, 842, 800, 755, 667, 610 cm^{-1} ; $[\alpha]_{\text{D}}^{25}=-2.1$ ($c=2.23$, CHCl_3); HRMS (ESI+) (m/z): $[M+\text{Na}]^+$ calcd for $\text{C}_{27}\text{H}_{46}\text{O}_9$: 537.3040; found: 537.3041.

Acknowledgments

The authors are grateful to the NIH (R01GM111476 and R35-GM-128830) for financial support.

Conflict of interest

The authors declare no conflict of interest.

Keywords: chiral phosphoric acids · cyclic ethers · epoxides · mupirocin · regioselectivity

- [1] J. Marco-Contelles, M. T. Molina, S. Anjum, *Chem. Rev.* **2004**, *104*, 2857.
- [2] K. M. Morgan, J. A. Ellis, J. Lee, A. Fulton, S. L. Wilson, P. S. Dupart, R. Dastoori, *J. Org. Chem.* **2013**, *78*, 4303.
- [3] T. Katsuki, K. B. Sharpless, *J. Am. Chem. Soc.* **1980**, *102*, 5974.
- [4] S. Chang, J. M. Galvin, E. N. Jacobsen, *J. Am. Chem. Soc.* **1994**, *116*, 6937.
- [5] W. Zhang, J. L. Loebach, S. R. Wilson, E. N. Jacobsen, *J. Am. Chem. Soc.* **1990**, *112*, 2801.
- [6] Z. X. Wang, Y. Tu, M. Frohn, J. R. Zhang, Y. Shi, *J. Am. Chem. Soc.* **1997**, *119*, 11224.
- [7] Y. Tu, Z. X. Wang, Y. Shi, *J. Am. Chem. Soc.* **1996**, *118*, 9806.
- [8] B. Das, K. Damodar, in *Heterocycles in Natural Product Synthesis* (Eds.: K. C. Majumdar, S. K. Chattopadhyay), Wiley-VCH, Weinheim, **2011**, 63–95.
- [9] A. Padwa, S. Murphree, *ARKIVOC (Gainesville, FL, U.S.)* **2006**, 2006, 6.
- [10] A. R. Gallimore, *Nat. Prod. Rep.* **2009**, *26*, 266.
- [11] D. E. Cane, W. D. Celmer, J. W. Westley, *J. Am. Chem. Soc.* **1983**, *105*, 3594.
- [12] K. Nakanishi, *Toxicon* **1985**, *23*, 473.
- [13] I. Vilotijevic, T. F. Jamison, *Science* **2007**, *317*, 1189.
- [14] a) Y. Shichijo, A. Migita, H. Oguri, M. Watanabe, T. Tokiwano, K. Watanabe, H. Oikawa, *J. Am. Chem. Soc.* **2008**, *130*, 12230; b) Y. Matsuura, Y. Shichijo, A. Minami, A. Migita, H. Oguri, M. Watanabe, T. Tokiwano, K. Watanabe, H. Oikawa, *Org. Lett.* **2010**, *12*, 2226.
- [15] J. E. Baldwin, *J. Chem. Soc. Chem. Commun.* **1976**, 0, 734.
- [16] I. Vilotijevic, T. F. Jamison, *Angew. Chem. Int. Ed.* **2009**, *48*, 5250; *Angew. Chem.* **2009**, *121*, 5352.
- [17] a) H. Matsukura, M. Morimoto, H. Koshino, T. Nakata, *Tetrahedron Lett.* **1997**, *38*, 5545; b) T. Suzuki, O. Sato, M. Hiram, *Tetrahedron Lett.* **1990**, *31*, 4747; c) K. C. Nicolaou, C. V. C. Prasad, P. K. Somers, C. K. Hwang, *J. Am. Chem. Soc.* **1989**, *111*, 5330; d) K. C. Nicolaou, M. E. Duggan, C. K. Hwang, P. K. Somers, *J. Chem. Soc. Chem. Commun.* **1985**, 0, 1359.
- [18] C. Mukai, Y. I. Sugimoto, Y. Ikeda, M. Hanaoka, *Tetrahedron* **1998**, *54*, 823.
- [19] a) Y. Morimoto, Y. Nishikawa, C. Ueba, T. Tanaka, *Angew. Chem. Int. Ed.* **2006**, *45*, 810; *Angew. Chem.* **2006**, *118*, 824; b) F. Bravo, F. E. McDonald, W. A. Neiwert, B. Do, K. I. Hardcastle, *Org. Lett.* **2003**, *5*, 2123.
- [20] a) T. P. Heffron, T. F. Jamison, *Org. Lett.* **2003**, *5*, 2339; b) G. Adiwidjaja, H. Flörke, A. Kirschning, E. Schaumann, *Tetrahedron Lett.* **1995**, *36*, 8771.
- [21] a) S. Sittihan, T. F. Jamison, *J. Am. Chem. Soc.* **2019**, *141*, 11239; b) E. H. Kelley, T. F. Jamison, *Bioorg. Med. Chem.* **2018**, *26*, 5327; c) L. C. Czabaniuk, T. F. Jamison, *Org. Lett.* **2015**, *17*, 774; d) J. A. Byers, T. F. Jamison, *Proc. Natl. Acad. Sci. USA* **2013**, *110*, 16724; e) J. J. Mousseau, C. J. Morten, T. F. Jamison, *Chem. Eur. J.* **2013**, *19*, 10004; f) B. S. Underwood, J. Tanuwidjaja, T. F. Jamison, *Tetrahedron* **2013**, *69*, 5205; g) C. J. Morten, J. A. Byers, A. R. Van Dyke, I. Vilotijevic, T. F. Jamison, *Chem. Soc. Rev.* **2009**, *38*, 3175; h) J. Tanuwidjaja, S.-S. Ng, T. F. Jamison, *J. Am. Chem. Soc.* **2009**, *131*, 12084; i) C. J. Morten, T. F. Jamison, *J. Am. Chem. Soc.* **2009**, *131*, 6678; j) J. A. Byers, T. F. Jamison, *J. Am. Chem. Soc.* **2009**, *131*, 6383; k) A. R. Van Dyke, T. F. Jamison, *Angew. Chem. Int. Ed.* **2009**, *48*, 4430; *Angew. Chem.* **2009**, *121*, 4494.
- [22] Selected examples of chiral catalyst-controlled functionalization of natural products: a) C. A. Lewis, S. J. Miller, *Angew. Chem. Int. Ed.* **2006**, *45*, 5616; *Angew. Chem.* **2006**, *118*, 5744; b) M. Sánchez-Roselló, A. L. A. Puchlopek, A. J. Morgan, S. J. Miller, *J. Org. Chem.* **2008**, *73*, 1774; c) C. A. Lewis, K. E. Longcore, S. J. Miller, P. A. Wender, *J. Nat. Prod.* **2009**, *72*,

- 1864; d) P. A. Jordan, S. J. Miller, *Angew. Chem. Int. Ed.* **2012**, *51*, 2907; *Angew. Chem.* **2012**, *124*, 2961; e) T. P. Pathak, S. J. Miller, *J. Am. Chem. Soc.* **2012**, *134*, 6120; f) B. S. Fowler, K. M. Laemmerhold, S. J. Miller, *J. Am. Chem. Soc.* **2012**, *134*, 9755; g) P. A. Lichtor, S. J. Miller, *Nat. Chem.* **2012**, *4*, 990; h) Y. Ueda, K. Mishiro, K. Yoshida, T. Furuta, T. Kawabata, *J. Org. Chem.* **2012**, *77*, 7850; i) T. P. Pathak, S. J. Miller, *J. Am. Chem. Soc.* **2013**, *135*, 8415; j) S. Han, S. J. Miller, *J. Am. Chem. Soc.* **2013**, *135*, 12414; k) X. Sun, H. Lee, S. Lee, K. L. Tan, *Nat. Chem.* **2013**, *5*, 790; l) S. Yoganathan, S. J. Miller, *J. Med. Chem.* **2015**, *58*, 2367; m) Y. Ueda, T. Furuta, T. Kawabata, *Angew. Chem. Int. Ed.* **2015**, *54*, 11966; *Angew. Chem.* **2015**, *127*, 12134; n) J. M. Howell, K. Feng, J. R. Clark, L. J. Trzepkowski, M. C. White, *J. Am. Chem. Soc.* **2015**, *137*, 14590; o) J. He, L. G. Hamann, H. M. L. Davies, R. E. J. Beckwith, *Nat. Commun.* **2015**, *6*, 5943; p) A. Sharma, J. F. Hartwig, *Nature* **2015**, *517*, 600; q) M. Yanagi, R. Nino-miya, Y. Ueda, T. Furuta, T. Yamada, T. Sunazuka, T. Kawabata, *Chem. Pharm. Bull.* **2016**, *64*, 907; r) R. R. Karimov, A. Sharma, J. F. Hartwig, *ACS Cent. Sci.* **2016**, *2*, 715; s) H. M. Key, S. J. Miller, *J. Am. Chem. Soc.* **2017**, *139*, 15460; t) J. Li, S. Grosslight, S. J. Miller, M. S. Sigman, F. D. Toste, *ACS Catal.* **2019**, *9*, 9794.
- [23] a) J. Lee, A. Borovika, Y. Khomutnyk, P. Nagorny, *Chem. Commun.* **2017**, *53*, 8976; b) J.-H. Tay, A. J. Arguelles, M. D. DeMars II, P. M. Zimmerman, D. H. Sherman, P. Nagorny, *J. Am. Chem. Soc.* **2017**, *139*, 8570; c) Y. Y. Khomutnyk, A. J. Arguelles, G. A. Winschel, Z. Sun, P. M. Zimmerman, P. Nagorny, *J. Am. Chem. Soc.* **2016**, *138*, 444; d) E. Mensah, N. Camasso, W. Kaplan, P. Nagorny, *Angew. Chem. Int. Ed.* **2013**, *52*, 12932; *Angew. Chem.* **2013**, *125*, 13170; e) P. Nagorny, Z. Sun, G. A. Winschel, *Synlett* **2013**, *24*, 661; f) Z. Sun, G. A. Winschel, A. Borovika, P. Nagorny, *J. Am. Chem. Soc.* **2012**, *134*, 8074.
- [24] Z. Wang, W. K. Law, J. Sun, *Org. Lett.* **2013**, *15*, 5964.
- [25] a) M. R. Monaco, S. Prévost, B. List, *Angew. Chem. Int. Ed.* **2014**, *53*, 8142; *Angew. Chem.* **2014**, *126*, 8280; b) S. Liao, M. Leutzsch, M. R. Monaco, B. List, *J. Am. Chem. Soc.* **2016**, *138*, 5230; c) M. R. Monaco, S. Prévost, B. List, *J. Am. Chem. Soc.* **2014**, *136*, 16982; d) M. R. Monaco, D. Fazzi, N. Tsuji, M. Leutzsch, S. Liao, W. Thiel, B. List, *J. Am. Chem. Soc.* **2016**, *138*, 14740.
- [26] a) P. M. Zimmerman, *J. Chem. Phys.* **2013**, *138*, 184102; b) P. M. Zimmerman, *J. Comput. Chem.* **2013**, *34*, 1385; c) P. M. Zimmerman, *J. Comput. Chem.* **2015**, *36*, 601; d) P. Zimmerman, *J. Chem. Theory Comput.* **2013**, *9*, 3043.
- [27] a) S. Khoshnood, M. Heidary, A. Asadi, S. Soleimani, M. Motahar, M. Savari, M. Saki, M. Abdi, *Biomed. Pharmacother.* **2019**, *109*, 1809; b) C. M. Thomas, J. Hothersall, C. L. Willis, T. J. Simpson, *Nat. Rev. Microbiol.* **2010**, *8*, 281; c) Y. J. Class, P. DeShong, *Chem. Rev.* **1995**, *95*, 1843; d) A. Ward, D. M. Campoli-Richards, *Drugs* **1986**, *32*, 425.
- [28] J. P. Clayton, R. S. Oliver, N. H. Rogers, *J. Chem. Soc. Perkin Trans. 1* **1979**, 838.
- [29] a) T. Akiyama, J. Itoh, K. Yokota, K. Fuchibe, *Angew. Chem. Int. Ed.* **2004**, *43*, 1566; *Angew. Chem.* **2004**, *116*, 1592; b) D. Uraguchi, M. Terada, *J. Am. Chem. Soc.* **2004**, *126*, 5356.
- [30] A. L. Dewyer, P. M. Zimmerman, *Org. Biomol. Chem.* **2017**, *15*, 501.
- [31] Z. Sun, G. A. Winschel, P. M. Zimmerman, P. Nagorny, *Angew. Chem. Int. Ed.* **2014**, *53*, 11194; *Angew. Chem.* **2014**, *126*, 11376.
- [32] Computational studies of related CPA-catalyzed transformations: a) P. A. Champagne, K. N. Houk, *J. Am. Chem. Soc.* **2016**, *138*, 12356; b) T. J. Seguin, S. E. Wheeler, *ACS Catal.* **2016**, *6*, 2681; c) R. Maji, P. A. Champagne, K. N. Houk, S. E. Wheeler, *ACS Catal.* **2017**, *7*, 7332; d) F. Duarte, R. S. Paton, *J. Am. Chem. Soc.* **2017**, *139*, 8886.
- [33] a) I. D. Gridnev, M. Kouchi, K. Sorimachi, M. Terada, *Tetrahedron Lett.* **2007**, *48*, 497; b) T. Marcelli, P. Hammar, F. Himo, *Chem. Eur. J.* **2008**, *14*, 8562.
- [34] Y. Shao, Z. Gan, E. Epifanovsky, A. T. B. Gilbert, M. Wormit, J. Kussmann, A. W. Lange, A. Behn, J. Deng, X. Feng, et al., *Mol. Phys.* **2015**, *113*, 184.
- [35] a) A. D. Becke, *J. Chem. Phys.* **1997**, *107*, 8554; b) S. Grimme, *J. Comput. Chem.* **2006**, *27*, 1787.
- [36] a) P. C. Hariharan, J. A. Pople, *Theor. Chim. Acta* **1973**, *28*, 213; b) M. M. Francl, W. J. Pietro, W. J. Hehre, J. S. Binkley, M. S. Gordon, D. J. DeFrees, J. A. Pople, *J. Chem. Phys.* **1982**, *77*, 3654.
- [37] A. V. Marenich, C. J. Cramer, D. G. Truhlar, *J. Phys. Chem. B* **2009**, *113*, 6378.
- [38] J. Da Chai, M. Head-Gordon, *J. Chem. Phys.* **2008**, *128*, 084106.

Manuscript received: November 18, 2019

Revised manuscript received: January 1, 2020

Accepted manuscript online: January 6, 2020

Version of record online: March 18, 2020